Tunnelling and Underground Space Technology 81 (2018) 289–295

Contents lists available at ScienceDirect

Tunnelling and Underground Space Technology

journal homepage: www.elsevier.com/locate/tust

Analytical estimation of stress distribution in interbedded layers and its implication to rockburst in strong layer

Jianping Yang[a], Weizhong Chen[a,b], Xianjun Tan[a], Diansen Yang[a,*]

[a] State Key Laboratory of Geomechanics and Geotechnical Engineering, Institute of Rock and Soil Mechanics, Chinese Academy of Sciences, 430071 Wuhan, PR China
[b] Research Center of Geotechnical and Structural Engineering, Shandong University, 250061 Jinan, PR China

ARTICLE INFO

Keywords:
Interbedded layer
Stress
Analytical
Rockburst
Tunnel

ABSTRACT

In-situ stress is one of the most important factors affecting the safety and stability of underground excavations. Past measurement results show that the magnitudes and directions of in- situ stresses vary substantially in different lithological formations. However, the relationship between stresses distribution and rock mechanical properties is still unclear. In this paper, the stress distribution in interbedded strong and weak layers was analytically studied based on linear elastic mechanics. Derived solutions were validated by comparison with Finite Element Method (FEM) results and field measurement results. Comparisons show that analytical results agree with the numerical results, and the maximum difference is less than 1%. The maximum difference between the analytical results and field measurements is 10.8%. Furthermore, the derived solution was used to evaluate the stress distribution in a geologically abnormal area in the Neelum-Jhelum (NJ) hydroplant project. Stress concentration state in strong layers changes as the strata change from sub-vertical to sub-horizontal, and the stress state in the sub-horizontal strata greatly favours rockburst according to the Turchaninov criterion. The change in stress concentration state might be the underlying reason for the severe rockburst in the abnormal structure area in the NJ project.

1. Introduction

Stress measurement and estimation of lithological formations is a key factor in evaluating the safety and stability of underground engineering, e.g., tunnels, underground caverns, mining and petroleum (Martin et al., 2003; Cai, 2011; Zuo et al., 2009; Wang et al., 2015). A significant number of studies have been carried out to estimate in situ stress (Evans et al., 1989; Amadei and Stephansson, 1997; Fairhurst, 2003; Zoback et al., 2003; Sjöberg and Klasson, 2003; Nelson and Hillis, 2005; Li et al., 2007; Wang et al., 2009; Xu et al., 2014; Bourne, 2003). Stress magnitudes and directions vary substantially in different lithological formations. The stress distribution in different rock formations depends on pore pressure, strength, Young's modulus, and the present-day stress state (Plumb, 1994; Reches, 1998; Nelson et al., 2006). For example, Plumb (Plumb, 1994) found that the ratio of minimum to vertical stress was 40% higher in hard carbonate rocks, and 20% higher in hard sandstones, than in the weak shales in compressional tectonic settings. Image logs from wells in the West Tuna area (Nelson et al., 2006) revealed that wellbore failure was restricted to relatively rigid sandstone and did not occur in the interbedded weak shales. Nelson et al. (Nelson et al., 2006) investigated this phenomenon using the Finite Element Method (FEM) and found that the stress concentration in strong sandstone plays an important role. From the FEM results, the maximum tangential stress in sandstone is 80 MPa and 25 MPa in shale. Stress focusing causes borehole breakout in the sandstone despite the higher uniaxial compressive strength (UCS = 60 MPa). Conversely, stresses are too low to generate wellbore failure in the relatively weak shales (UCS = 30 MPa). Therefore, a better understanding of stress distribution is necessary to estimate the safety of the engineering in interbedded formations.

In engineering projects, the stress is seldom measured in all lithological units due to time and budget limitations. In many situations associated with deep excavation, it may be impossible to measure the stress state in some strata due to several factors, e.g., soft rock creep/relaxation, or borehole overbreak. However, the in-situ stress needs to be estimated to help the design and assess the risk of underground excavation. Until now, there is still no simple method to rapidly estimate stress distribution in interbedded strong and weak layers.

In this study, an analytical method for determining the 3D stress distribution in an interbedded formation is proposed and validated using FEM analysis and field results. This method is employed to analyze the stress distribution in a geologically abnormal area where the

* Corresponding author.
E-mail address: dsyang@whrsm.ac.cn (D. Yang).

https://doi.org/10.1016/j.tust.2018.07.007
Received 14 July 2017; Received in revised form 6 May 2018; Accepted 7 July 2018

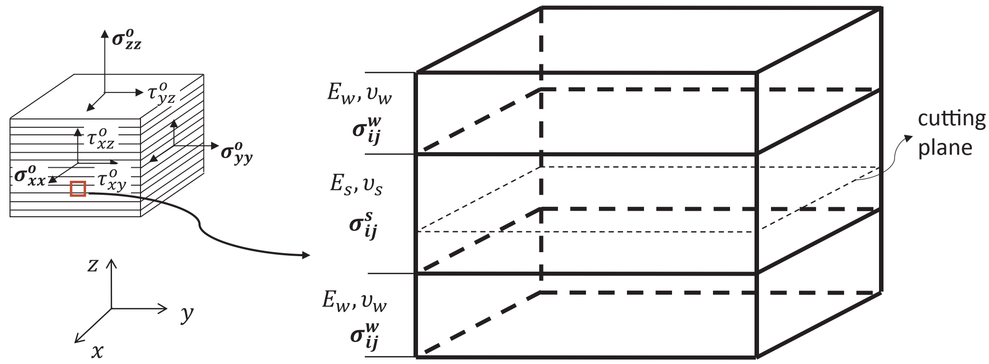

Fig. 1. Schematic diagram of interbedded strong and weak layers.

strata quickly change from a sub-vertical to sub-horizontal orientation. The cause of a severe rockburst in the abnormal area is explained from the aspect of stress concentration.

2. Analytical stress distribution in interbedded layers

A representative interbedded layer model is chosen and illustrated in Fig. 1. The bedding plane of the formation is parallel with the xy plane. To simplify the analysis, the following assumptions are adopted: (1) the layer's dimensions in the x and y directions are extremely large compared to the layer thickness; (2) rocks are isotropic and homogenous; (3) linear elastic theory is valid.

From the assumptions, we can infer that the stress components in the cutting plane, i.e. parallel with the bedding plane, are uniform: the values of σ_{xx}, σ_{yy}, σ_{zz}, τ_{xy}, τ_{xz} and τ_{yz} are the same at any two points in the same cutting plane.

2.1. Stress analysis

For a body enclosed by two cutting planes parallel to the xy plane, the forces F_x, F_y, and F_z on the two cutting planes are equal and in opposite directions based on the static equilibrium equation. So, τ_{xz}, τ_{yz}, and σ_{zz} in any two parallel planes are the same because the stress components in the cutting plane are uniform as indicated before. Thus,

$$\sigma^w_{zz} = \sigma^s_{zz} \tag{1}$$

$$\tau^w_{xz} = \tau^s_{xz} \tag{2}$$

$$\tau^w_{yz} = \tau^s_{yz} \tag{3}$$

Stress component superscripts denote rock type, s denotes a strong layer and w denotes a weak layer. The self-weight stress increment is not considered in σ_{zz}, because the value is commonly negligible in formations that are tens-of-meters thick compared with the absolute vertical stress σ_{zz}.

2.2. Strain analysis

As a homogeneous medium, the uniform σ_{xx}, σ_{yy}, and τ_{xy} at any points on the cutting plane (parallel with xy plane) will induce the uniform strains (ε_{xx}, ε_{yy}, and ε_{xy}). Moreover, strain components (ε_{xx}, ε_{yy}, and ε_{xy}) should be the same in adjacent cutting planes due to the continuous condition. Thus, strain components ε_{xx}, ε_{yy}, and ε_{xy} are inferred to be uniform in different layers,

$$\varepsilon^w_{xx} = \varepsilon^s_{xx} \tag{4}$$

$$\varepsilon^w_{yy} = \varepsilon^s_{yy} \tag{5}$$

$$\varepsilon^w_{xy} = \varepsilon^s_{xy} \tag{6}$$

Applying Hook's law, Eqs. (4)–(6) can be written as,

$$\frac{1}{E_w}[\sigma^w_{xx} - \upsilon_w(\sigma^w_{yy} + \sigma^w_{zz})] = \frac{1}{E_s}[\sigma^s_{xx} - \upsilon_s(\sigma^s_{yy} + \sigma^s_{zz})] \tag{7}$$

$$\frac{1}{E_w}[\sigma^w_{yy} - \upsilon_w(\sigma^w_{xx} + \sigma^w_{zz})] = \frac{1}{E_s}[\sigma^s_{yy} - \upsilon_s(\sigma^s_{xx} + \sigma^s_{zz})] \tag{8}$$

$$\frac{\tau^w_{xy}}{2G_w} = \frac{\tau^s_{xy}}{2G_s} \tag{9}$$

When the stress in the strong layer is obtained through field stress measurements, the stress in the weak layer can be obtained as follows by solving Eqs. (7)–(9).

$$\sigma^w_{xx} = \frac{\frac{E_w}{E_s}[(1-\upsilon_s\upsilon_w)\sigma^s_{xx} - (\upsilon_s-\upsilon_w)\sigma^s_{yy} - \upsilon_s(1+\upsilon_w)\sigma^s_{zz}] + \upsilon_w(1+\upsilon_w)\sigma^w_{zz}}{1-(\upsilon_w)^2} \tag{10}$$

$$\sigma^w_{yy} = \frac{\frac{E_w}{E_s}[(1-\upsilon_s\upsilon_w)\sigma^s_{yy} - (\upsilon_s-\upsilon_w)\sigma^s_{xx} - \upsilon_s(1+\upsilon_w)\sigma^s_{zz}] + \upsilon_w(1+\upsilon_w)\sigma^w_{zz}}{1-(\upsilon_w)^2} \tag{11}$$

$$\tau^w_{xy} = \frac{E_w(1+\upsilon_s)}{E_s(1+\upsilon_w)}\tau^s_{xy} \tag{12}$$

Example. For a package of interbedded layers oriented as illustrated in Fig. 1, the mechanical parameters of the strong layer and weak layer are: $E_s = 20$ GPa, $\upsilon_s = 0.25$ and $E_w = 5$ GPa, $\upsilon_w = 0.3$ respectively. The stress measured in the strong rock is, $\sigma^s_{xx} = -65.3$ MPa, $\sigma^s_{yy} = -42.9$ MPa, $\sigma^s_{zz} = -37.5$ MPa, $\tau^s_{xy} = 23.3$ MPa, $\tau^s_{yz} = 1.1$ MPa and $\tau^s_{xz} = -10.8$ MPa.

The stress in the nearby weak layer can be obtained from Eqs. (1)–(3) and Eqs. (10)–(12),

$$\sigma^w_{xx} = -29.9 \text{ MPa} \quad \sigma^w_{yy} = -24.5 \text{ MPa}$$

$$\sigma^w_{zz} = -37.5 \text{ MPa}$$

$$\tau^w_{xy} = 5.6 \text{ MPa}$$

$$\tau^w_{yz} = 1.1 \text{ MPa}$$

$$\tau^w_{xz} = -10.8 \text{ MPa}$$

3. Verification of the analytical method using FEM modelling and field results

3.1. Verification by FEM modelling

3.1.1. FEM model

The dimensions of the FEM model in the x, y, and z directions are 300 m × 300 m × 360 m. The thickness of each layer is 12 m. The mechanical parameters of strong and weak layers are the same as in the